Electronic Supplementary Material (ESI) for Journal of Materials Chemistry A.
This journal is © The Royal Society of Chemistry 2020

**Electronic Supplementary Information**

# Coupled Conductor of Ionic Liquid with $Ti_3C_2$ MXene to Promote Electrochemical Properties

*Fangfang Yan,*[a,b] *Chuan Zhang,*[a] *Haiyan Wang,*[a] *Xiaguang Zhang,*[a] *Hucheng Zhang,*[*a] *Huanli Jia,*[a,b] *Yang Zhao,*[a] *Jianji Wang*[* a]

[a] Collaborative Innovation Centre of Henan Province for Green Manufacturing of Fine Chemicals, Key Laboratory of Green Chemical Media and Reactions, Ministry of Education, School of Chemistry and Chemical Engineering, Henan Normal University, Xinxiang, Henan 453007, China .Email: hzhang@htu.edu.cn; jwang@htu.edu.cn.

[b] School of 3D printing, Xinxiang University, Xinxiang, Henan 453003, P. R. China.

* Corresponding author. e-mail: hzhang@htu.edu.cn (H.Z); jwang@htu.edu.cn (J.W.)

## S1. Chemicals.

Titanium [Ti, Macklin, CAS#: 7440-32-6], Aluminum [Al, Aladdin, CAS#: 7429-90-5], Graphite [C, Aladdin, CAS#: 7782-42-5], 1-ethyl-3-methylimidazolium hexafluorophosphate (EmimPF6) [$C_6H_{11}N_2PF_6$, Lanzhou Greenchem ILs, CAS#: 155371-19-0], 1-ethyl-3-methylimidazolium hydrosulfate (EmimHSO4) [$C_6H_{12}N_2O_4S$ , Lanzhou Greenchem ILs, CAS#: 412009-61-1], Hydrofluoric acid [HF, Aladdin, CAS#: 7664-39-3]. Hydrochloric acid [HCl, Sinopharm, CAS#: 7647-01-0]. Nafion [5%, DuPont] were used without further purification.

## S2. Characterization Methods

X-ray diffraction (XRD) measures were conducted with X-ray diffraction (Bruker D8 Advance) using Cu $K_{\alpha 1}$ radiation (1.54056 Å) with 0.02 increment and 0.1s per step. UV-Visible (UV-vis) spectrum was performed on a UV-vis spectrophotometer (TU-1810). X-ray photoelectron spectroscopy (XPS) analysis was completed on an ESCALAB 250Xi spectrometer with Al Kα X-ray source (10 mA, 15 kV). The morphologies of $Ti_3C_2T_x$ flakes were analyzed by transmission electron microscope (TEM) (JEM 2100), in which the samples were prepared by dropping dilute aqueous colloidal solution of $Ti_3C_2T_x$ on normal carbon-support membrane. The average size of $Ti_3C_2T_x$ flakes were calculated from TEM images of 100 flakes. The scanning electron microscope (SEM) and Energy dispersive X-ray spectroscopy (EDS) analysis were performed on a field emission scanning electron microscopy (FEI Quanta FEG 250). After the dilute $Ti_3C_2T_x$ colloidal solution was cast on mica sheet, the thickness of $Ti_3C_2T_x$ flakes was carried out on an atomic force microscopy (AFM, MultiMode 8) in a contact and tapping modes. The Nanoscope Analysis software was used to analyze AFM data. The Raman spectra was obtained from Raman experimental system (LabRAM HR Evolution) with the laser source at 532 nm.

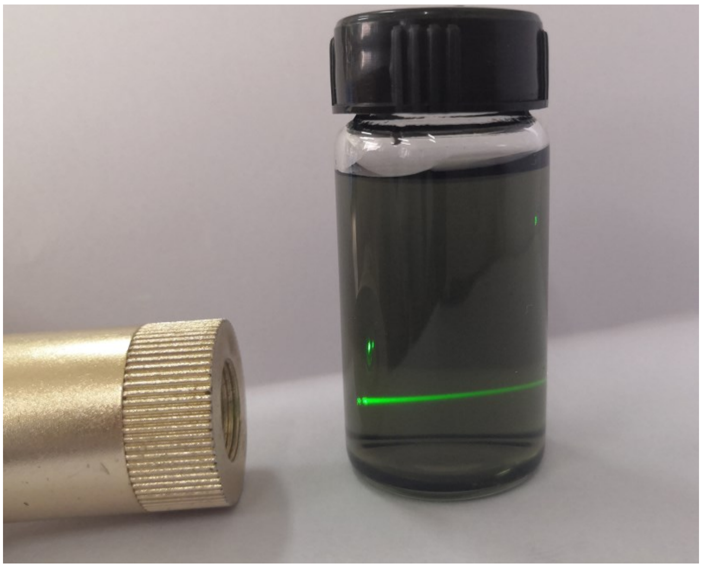

**Figure S1.** Tyndall effect of the dilute aqueous IL-$Ti_3C_2T_x$ colloidal solution.

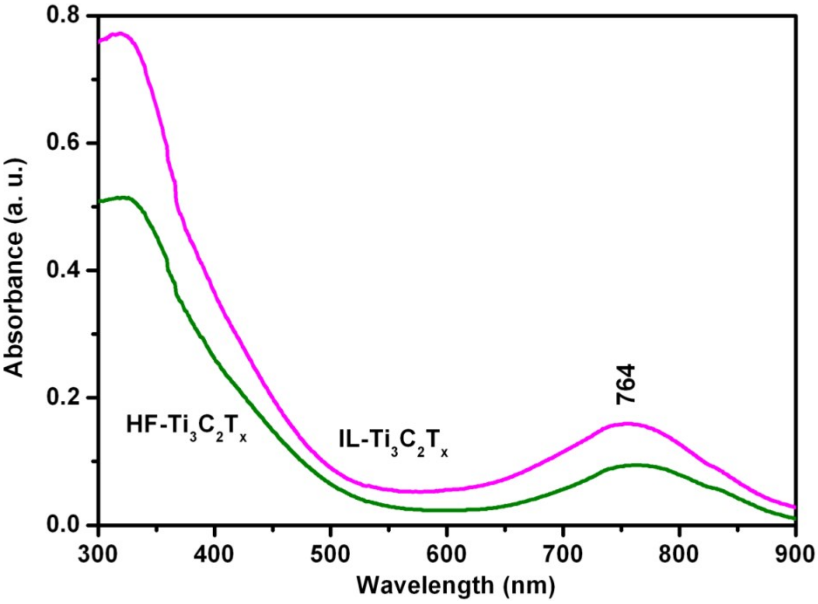


**Figure S2.** Ultraviolet-visible absorption spectra of IL-$Ti_3C_2T_x$ and HF-$Ti_3C_2T_x$ colloidal aqueous solutions, respectively.

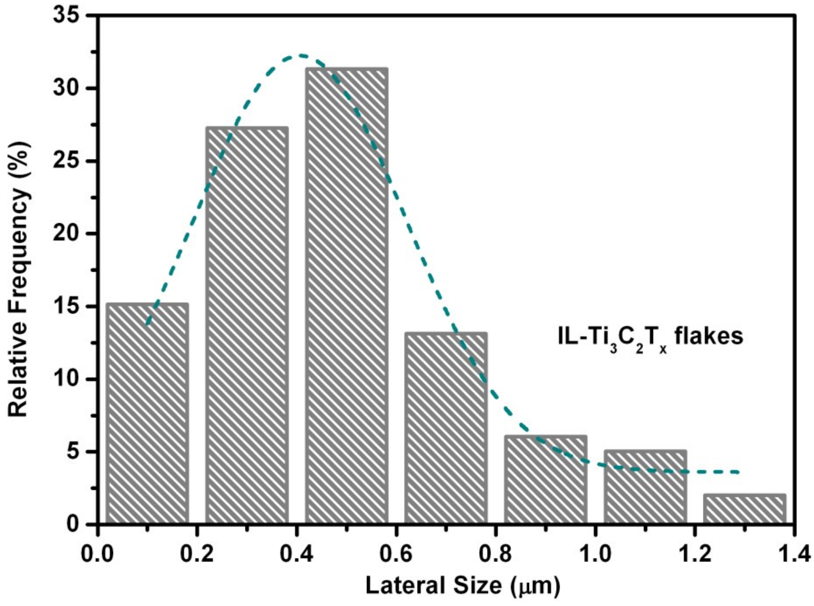


**Figure S3.** Lateral size distribution of IL-$Ti_3C_2T_x$ flakes.

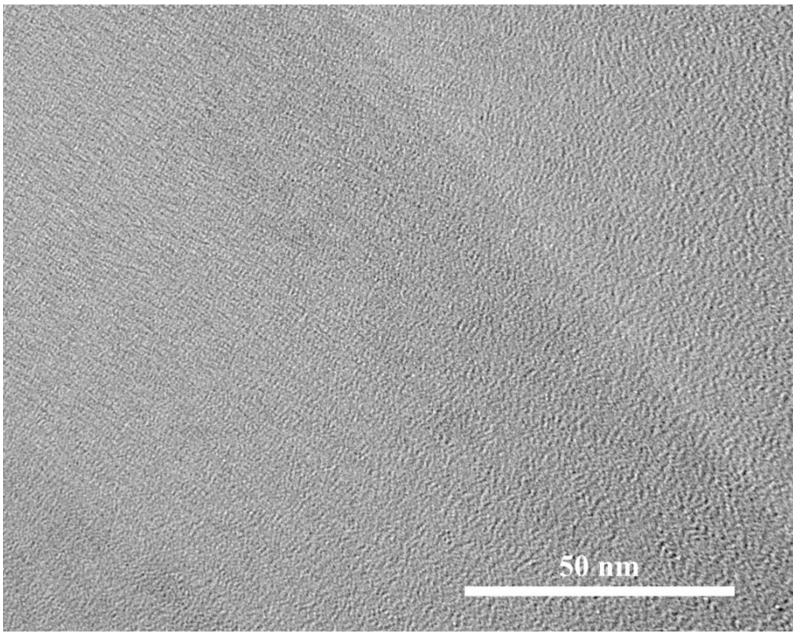


**Figure S4.** TEM images of IL-$Ti_3C_2T_x$ flakes at larger magnification. No obvious surface defects are discovered.

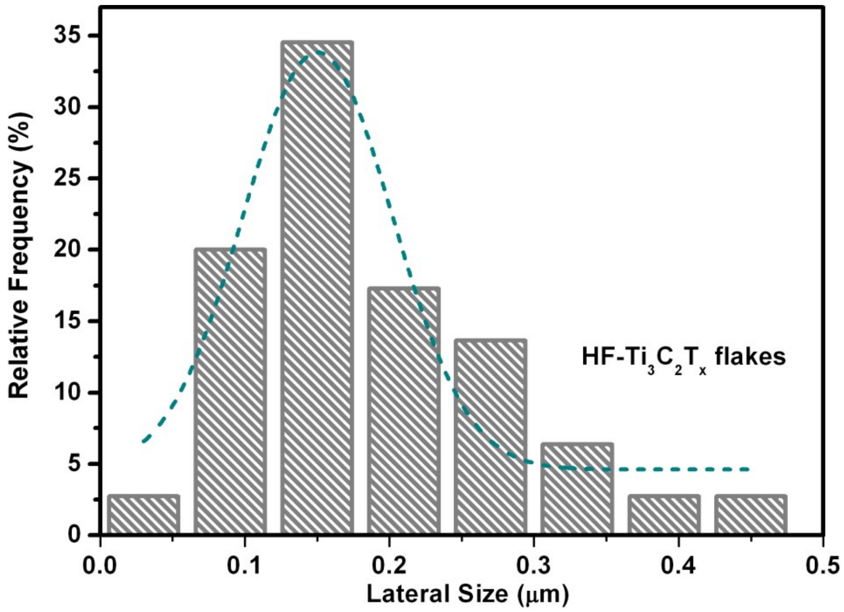


**Figure S5.** Lateral size distribution of HF-$Ti_3C_2T_x$ flakes.

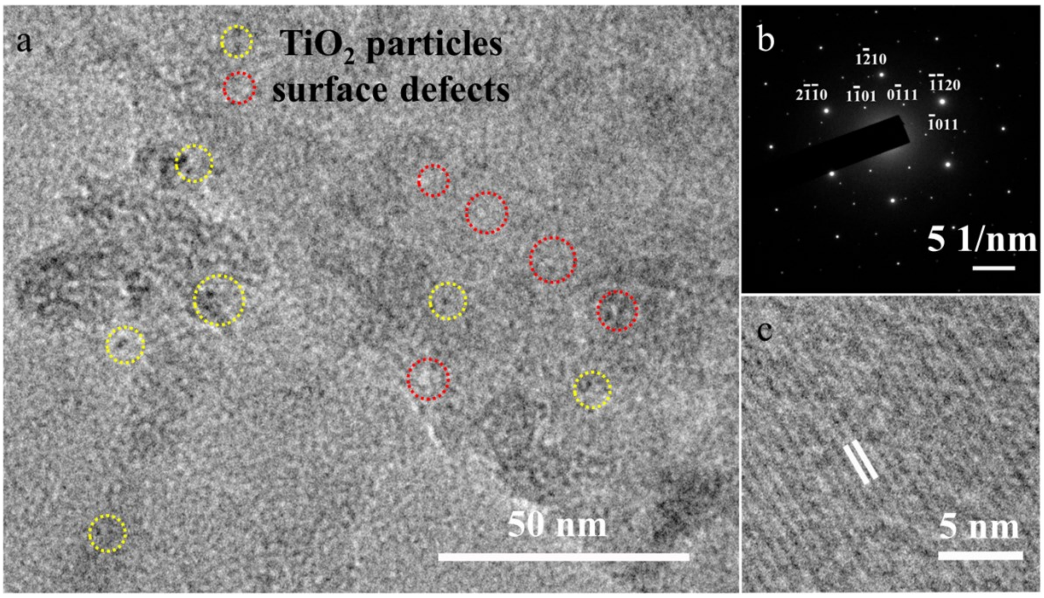


**Figure S6. a-c** TEM images at larger magnification **(a)**, SAED patterns **(b)**, HRTEM images **(c)** for HF-$Ti_3C_2T_x$ flakes.

**a**

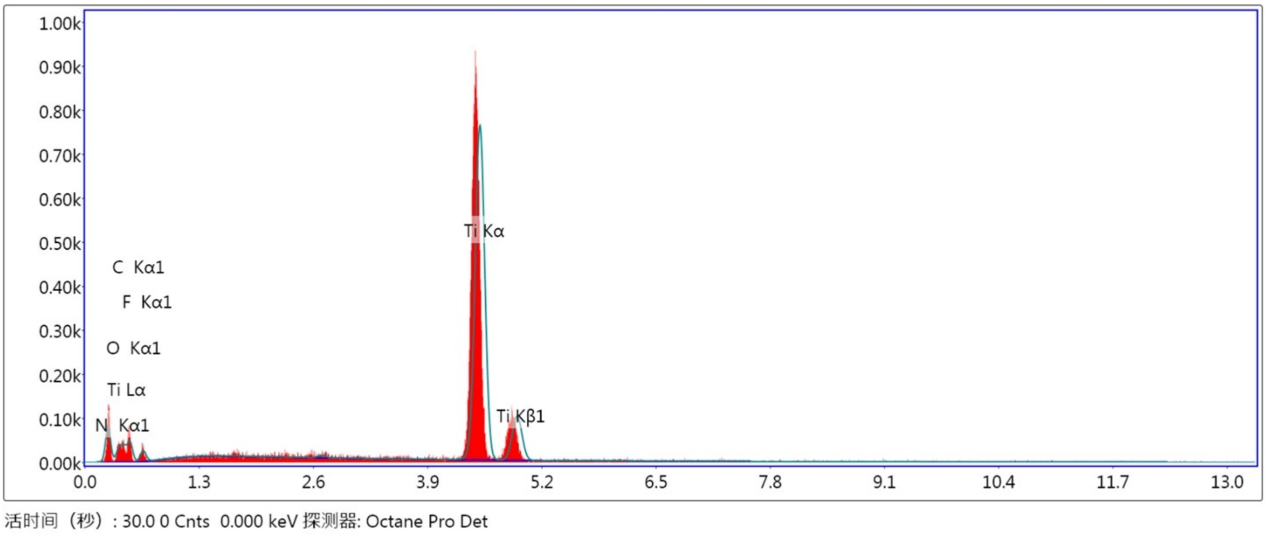


**b**

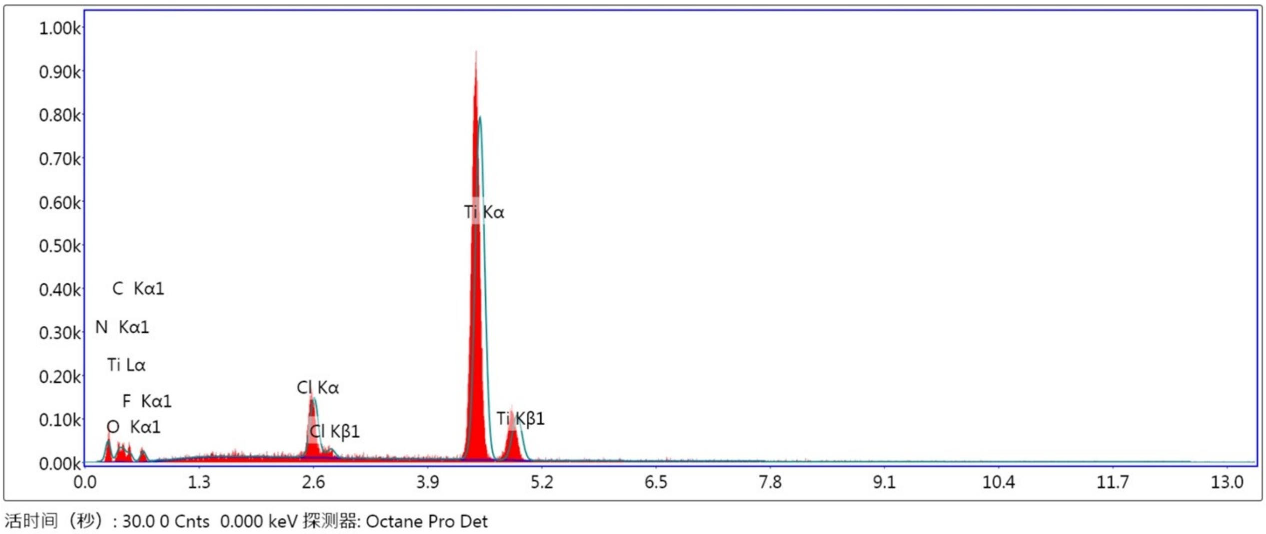


**FigureS7. a-b** Energy-dispersive spectra of HF-$Ti_3C_2T_x$ flakes **(a)**, and IL-$Ti_3C_2T_x$ flakes **(b)**.

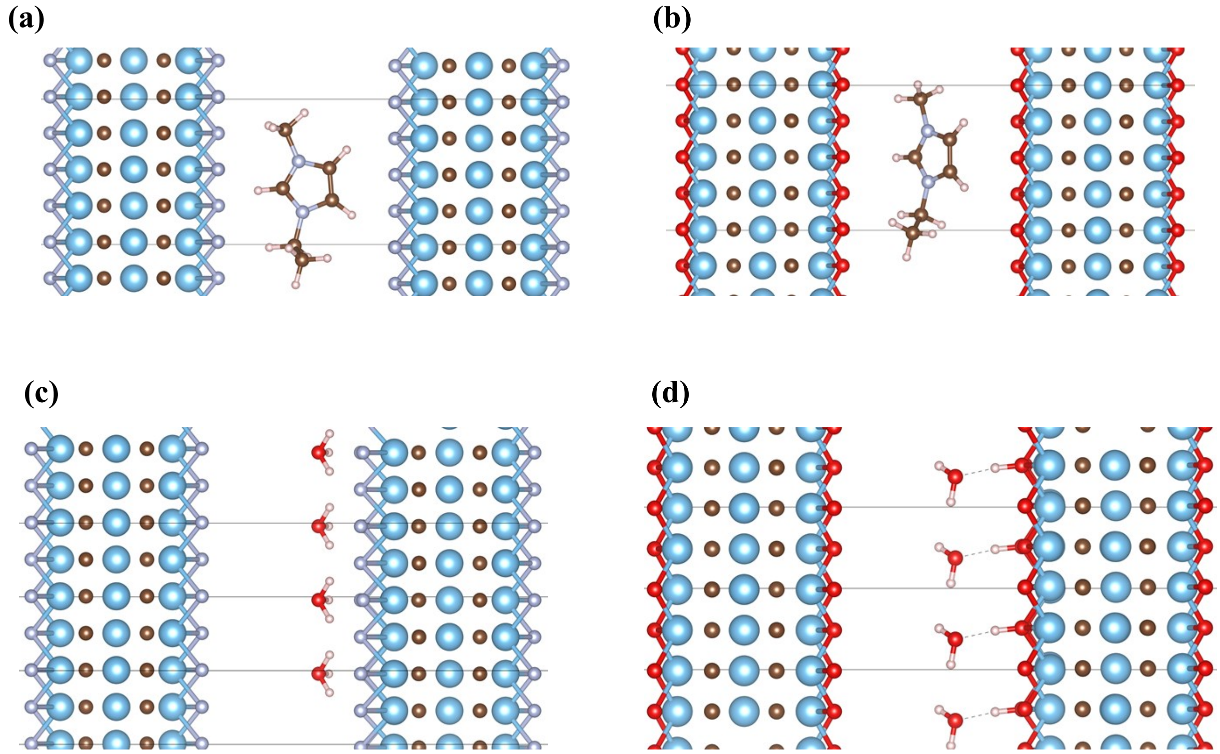


**Figure S8.** The optimized geometries of a [Emim]$^+$ **(a, b)** and 4 $H_3O^+$ **(c, d)** cations confined between two monolayers of $Ti_3C_2F_2$ **(a, c)** and $Ti_3C_2O_2$ **(b, d)**, respectively. The d spacing is set at 12.6 Å, and the blue, brown, magenta, grey, red and dark grey balls donate Ti, C, H, N, O and F atoms, respectively.

(a)

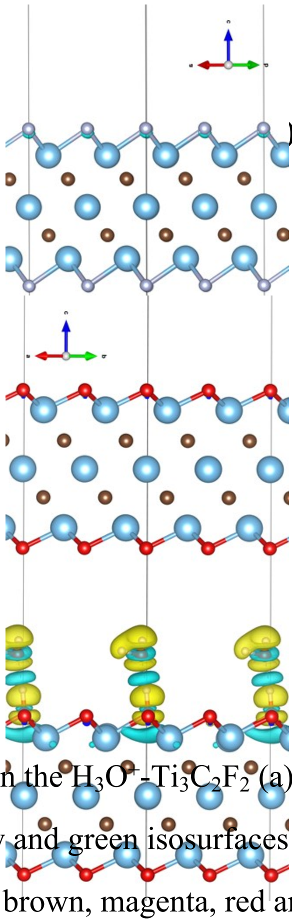

**Figure S9.** Charge density difference in the $H_3O^+$-$Ti_3C_2F_2$ (a), and $H_3O^+$-$Ti_3C_2O_2$ (b). The d spacing is set at 12.6 Å, and the yellow and green isosurfaces respectively denote the electron accumulation and depletion. The blue, brown, magenta, red and dark grey balls respectively denote Ti, C, H, O and F atoms.

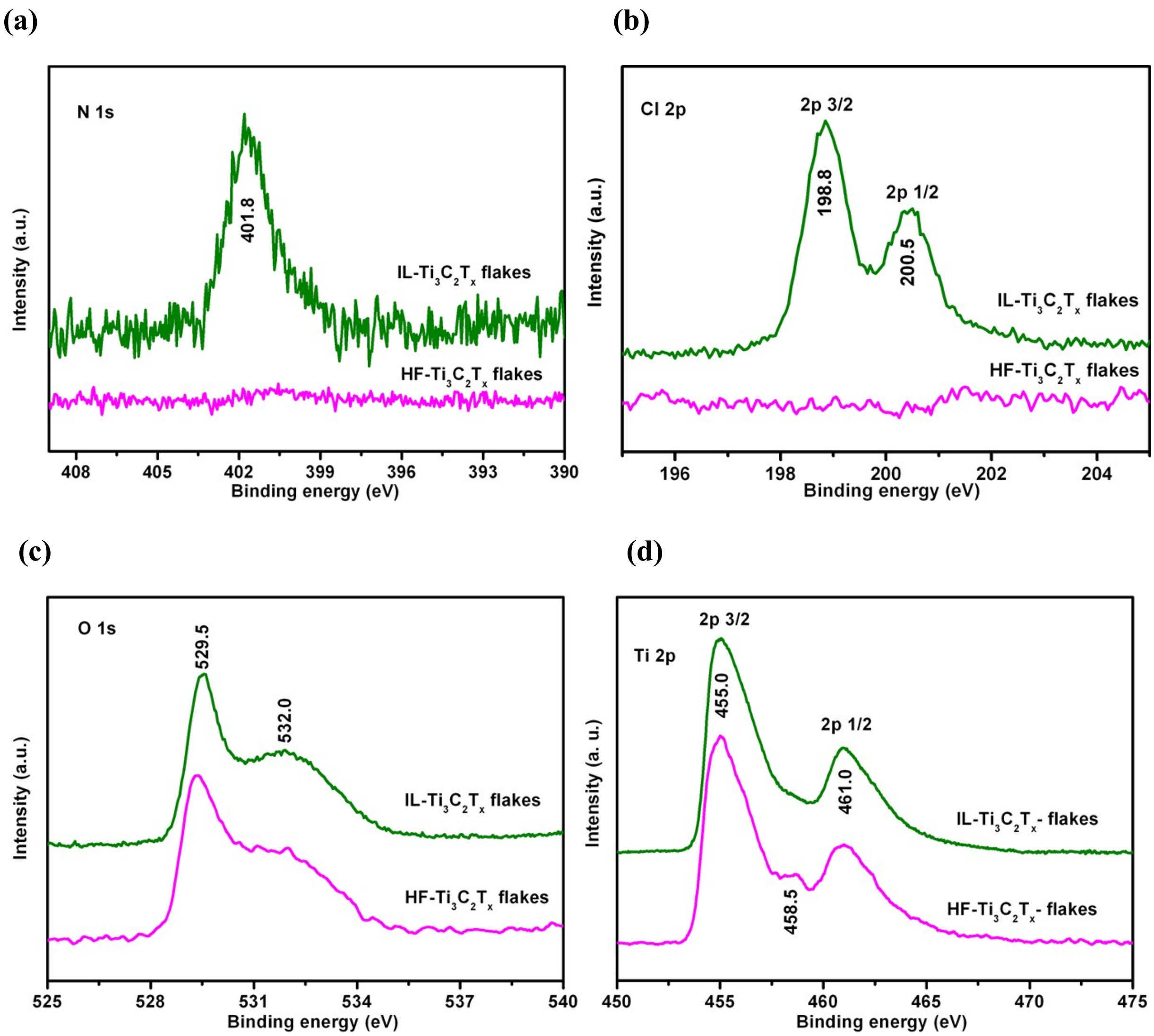


**Figure S10. a-d** High-resolution XPS spectra of N 1s (**a**), Cl 2p (**b**), O 1s (**c**), Ti 2p (**d**) in $Ti_3C_2T_x$ flakes.

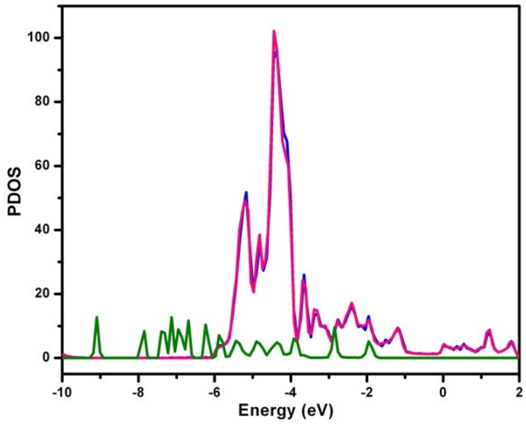


**Figure S11.** PDOS of O atoms (blue) in $Ti_3C_2O_2$, O atoms (pink) and $[Emim]^+$ (green) in $[Emim]^+$-$Ti_3C_2O_2$. The Fermi levels are set to zero.

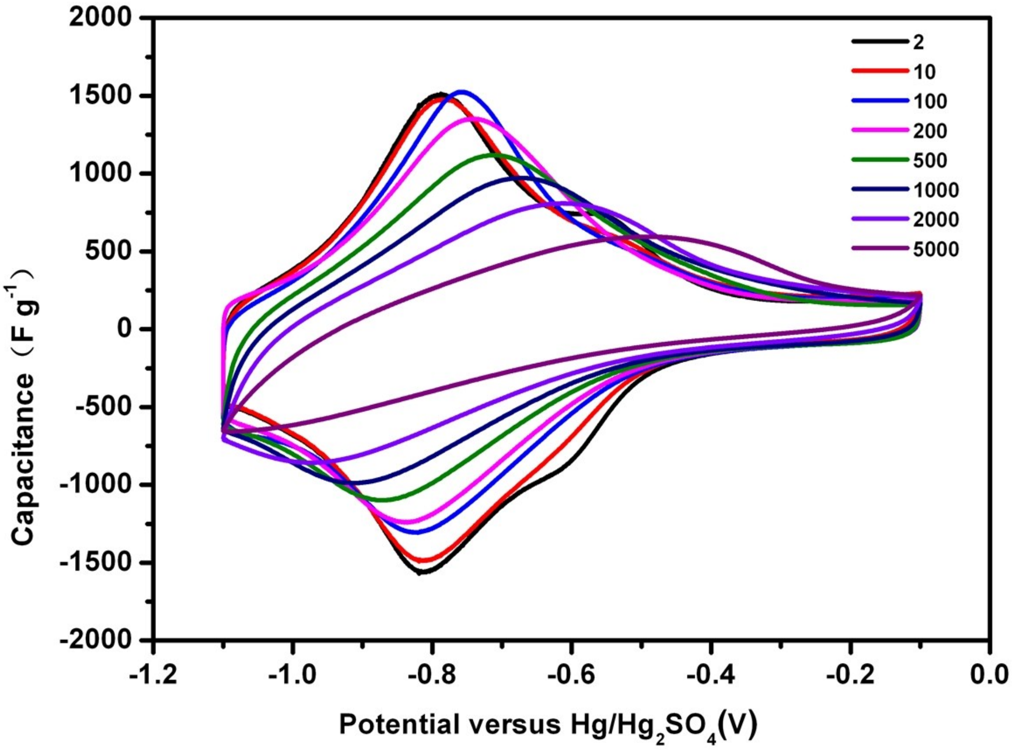


**Figure S12.** CVs of 0.05-IL-$Ti_3C_2T_x$/GCE in the 3M $H_2SO_4$-0.8M [Emim]$HSO_4$ electrolyte collected at scan rates from 10 to 5000mV $s^{-1}$.

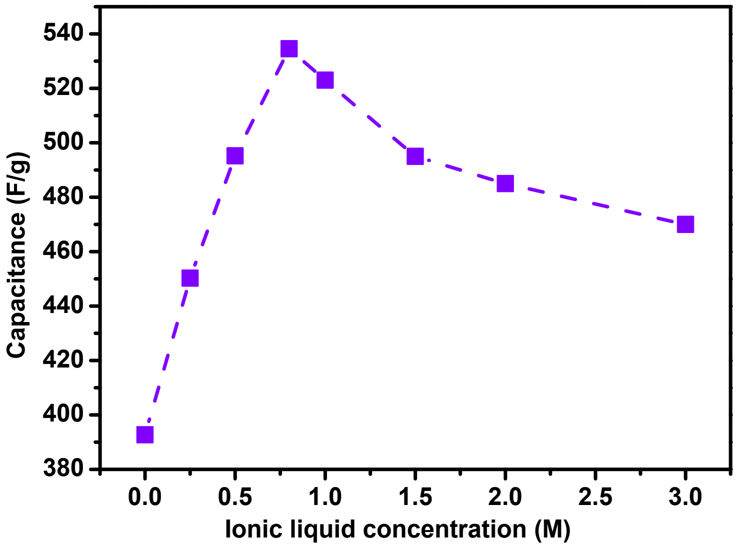


**Figure S13.** Capacitances of 1.7-IL-$Ti_3C_2T_x$/GCE measured at the scan rate of 2 mV $s^{-1}$ in 3M $H_2SO_4$ containing different [Emim]$HSO_4$ contents.

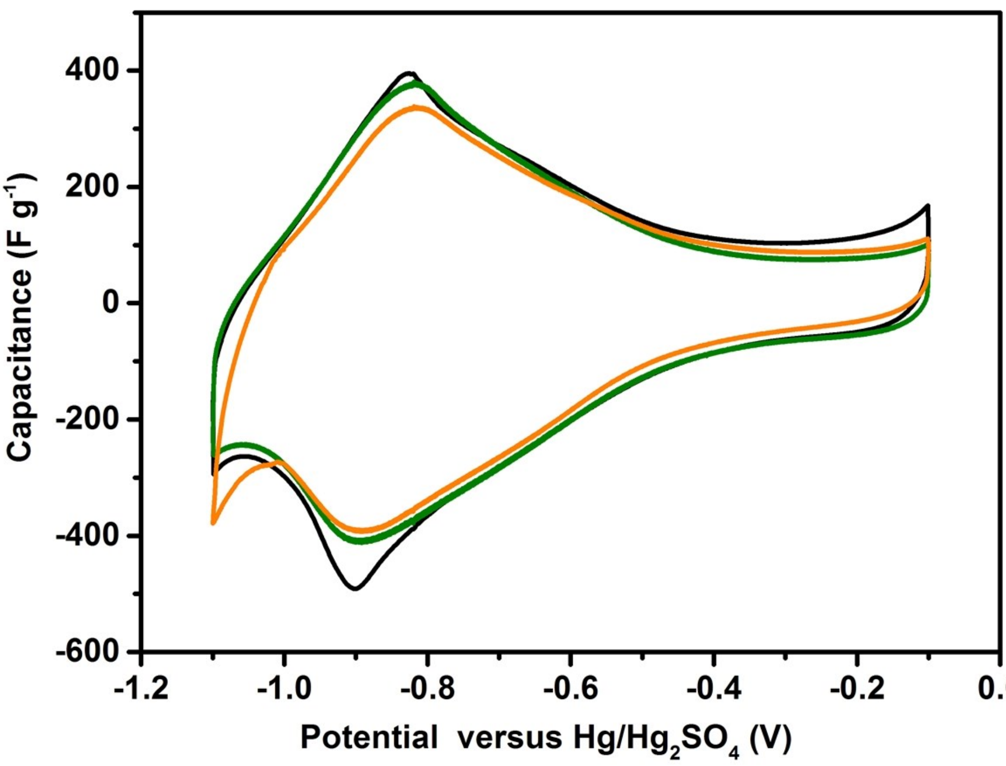


**Figure S14.** CVs of 1.7-HF-$Ti_3C_2T_x$/GCE recorded at the scan rate of 2 mV $s^{-1}$ in 3M $H_2SO_4$-0.8M [Emim]$HSO_4$. Initial CV (black), CV after the electrode was immersed in the electrolyte for 24 h (green), and CV after 100 cycles (yellow).

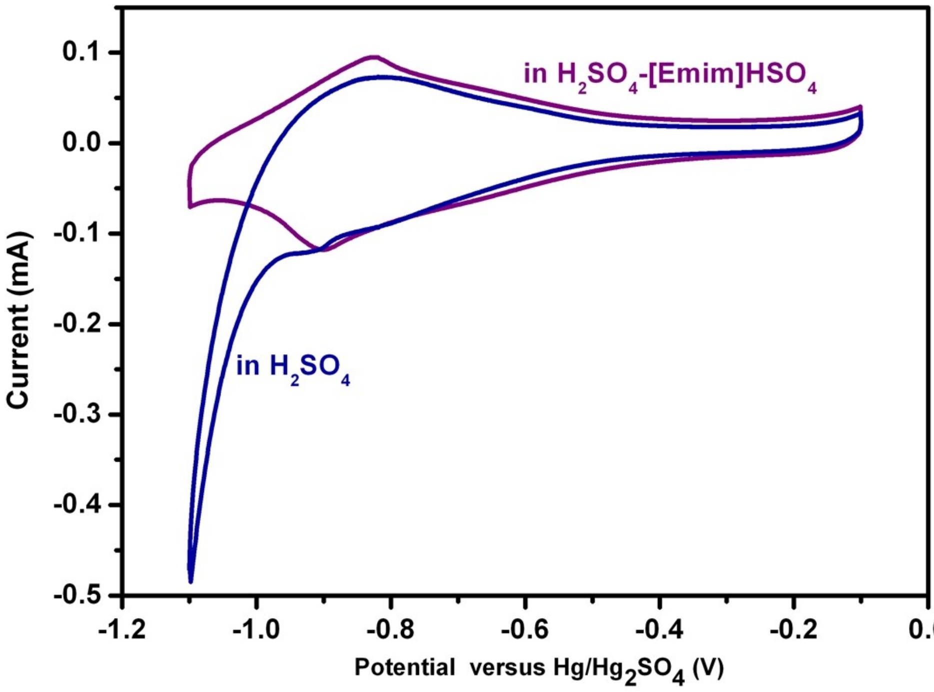


**Figure S15.** CVs of 1.7-HF-$Ti_3C_2T_x$/GCE recorded at the scan rate of 2 mV $s^{-1}$ in 3M $H_2SO_4$ and 3M $H_2SO_4$-0.8M [Emim]$HSO_4$, respectively.

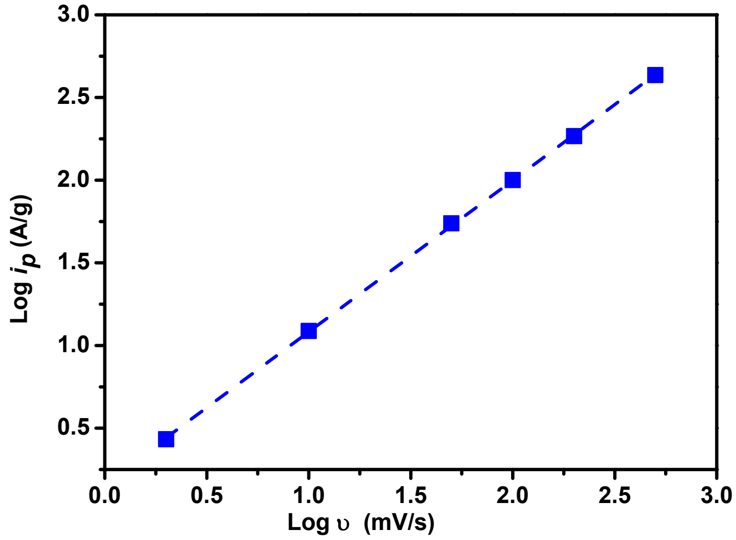


**Figure S16.** Peak current versus scan rate in the logarithm-logarithm graph for 1.7-IL-$Ti_3C_2T_x$/GCE in the mixed electrolyte.

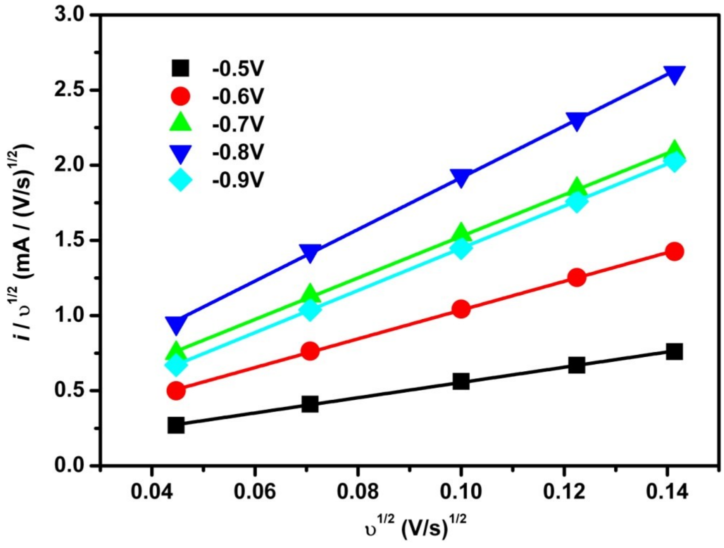


**Figure S17.** Dependence of $i/\upsilon^{1/2}$ on $\upsilon^{1/2}$ respectively at the defferent potentials in the CVs of IL-$Ti_3C_2T_x$ in the mixed electrolyte. Sweep rates were varied from 2 to 20 mV $s^{-1}$.

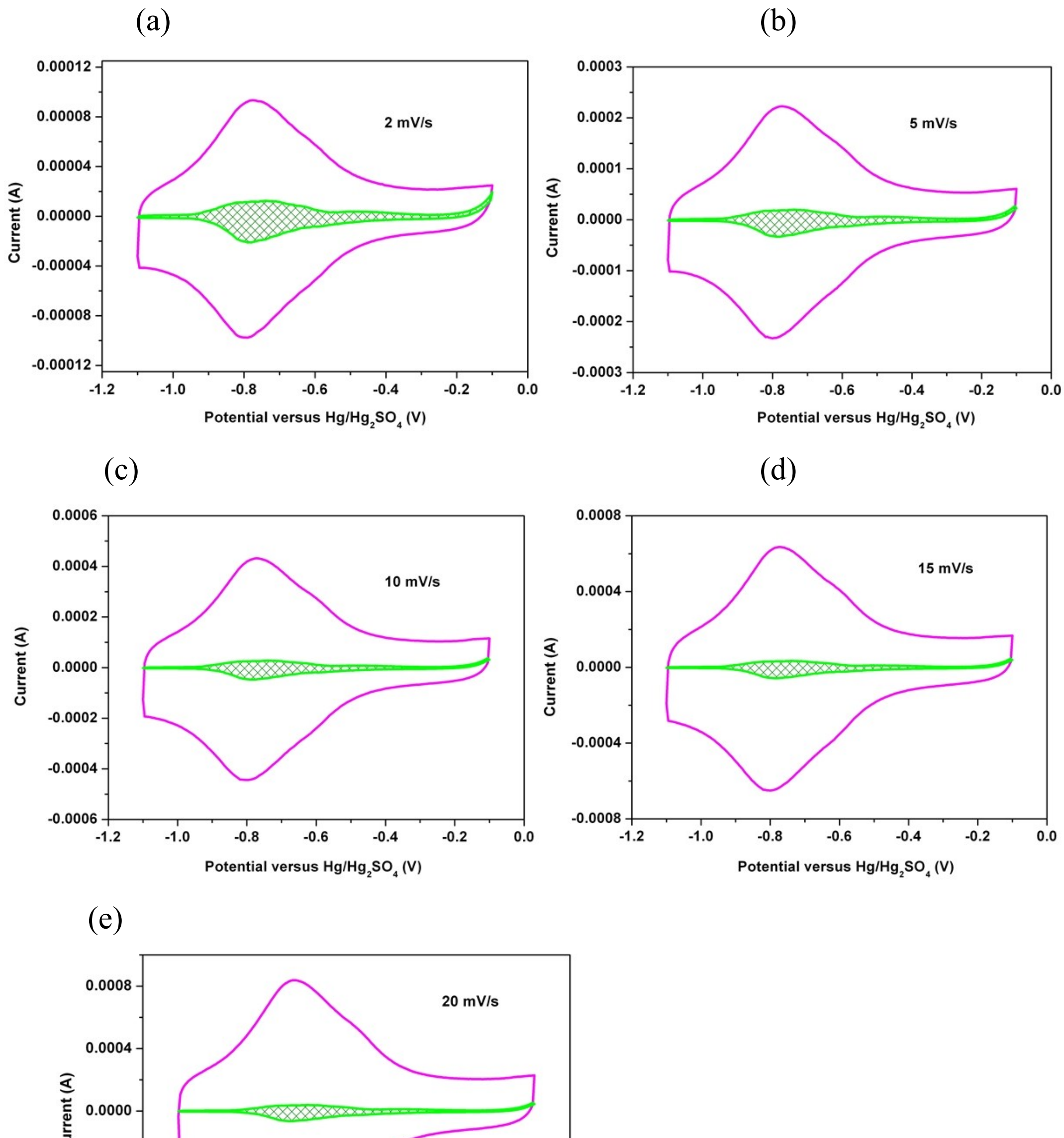


**Figure S18.** CVs of the IL-$Ti_3C_2T_x$ electrodes in the mixed electrolyte collected at 2, 5, 10, 15, and 20 mV $s^{-1}$. The CV profiles are separated into the contributions of diffusion- controlled capacitance (shaded regions) and surface controlled capacitance (unshaded region).

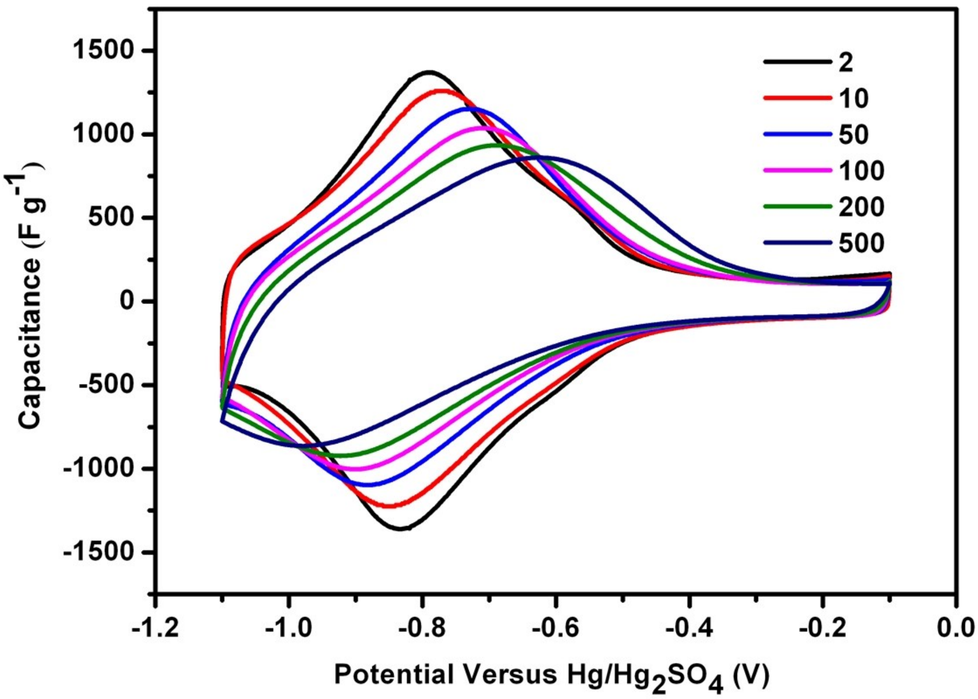


**Figure S19.** CVs of 1.7-IL-$Ti_3C_2T_x$/GCE in mixed electrolyte at the scan rates from 2 to 500 mV $s^{-1}$.

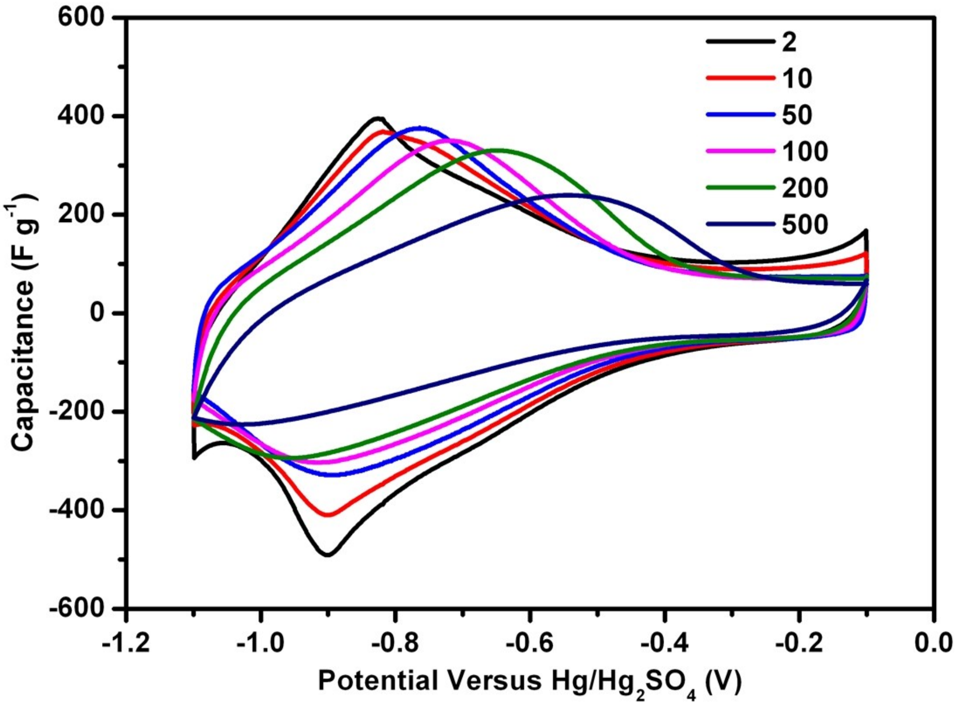


**Figure S20.** CVs of 1.7-HF-$Ti_3C_2T_x$/GCE in mixed electrolyte at the scan rates from 2 to 500 mV $s^{-1}$.

**Table S1.** Element contents (at.%) in HF-$Ti_3C_2T_x$ flakes and [Emim]-$Ti_3C_2T_x$ flakes.

| Sample | Ti | C | O | F | N | Cl |
|---|---|---|---|---|---|---|
| HF-$Ti_3C_2T_x$ flakes | 32.79 | 29.12 | 28.39 | 9.67 | 0.03 | 0.00 |
| [Emim]-$Ti_3C_2T_x$ flakes | 40.61 | 29.10 | 15.28 | 9.32 | 1.05 | 4.64 |

**Table S2.** Electronegativity of element in the terminal groups.

| F | O | H | Cl |
|---|---|---|---|
| 3.98 | 3.44 | 2.20 | 3.16 |

**Table S3.** Summary of the reported capacitive performances of $Ti_3C_2T_x$ MXene.

| Electrode | Mass loading ($mg{\cdot}cm^{-2}$) | Electrolyte | $C_g$* ($F{\cdot}g^{-1}$) | Scan rate or Discharge density | Cycling number /$C_g$ retention | Ref. |
|---|---|---|---|---|---|---|
| 1.7-IL-$Ti_3C_2T_x$ | 1.7 | 3M $H_2SO_4$-0.8M IL | 535 | $2mV{\cdot}S^{-1}$ | 10,000 /100% | This work |
| 13μm $Ti_3C_2T_x$ hydrogel film | 5.3 | 3M $H_2SO_4$ | 370 | $2mV{\cdot}S^{-1}$ | 10,000 /90% | 1 |
| 400-KOH-$Ti_3C_2$ | 0.5 | 1M $H_2SO_4$ | 500 | $1mV{\cdot}S^{-1}$ | 10,000 /99% | 2 |
| $Ti_3C_2T_x$ films | N/A | 1M $H_2SO_4$ | 245 | $2mV{\cdot}S^{-1}$ | 10,000 /100% | 3 |
| 52μm $Ti_3C_2T_x$ film | 8.48 | 1M $H_2SO_4$ | 314 | $2mV{\cdot}S^{-1}$ | 10,000 /89.1% | 4 |
| (MXene/TAEA*)$_{20}$ | N/A | PVA*/$H_2SO_4$ | 165 | $2mV\ S^{-1}$ | 10,000 /90.3% | 5 |
| $Ti_3C_2T_x$ hydrogel film | 4 | EMI-TFSI* | 70 | $20mV{\cdot}S^{-1}$ | 1,000 /80% | 6 |
| Binder-free $Ti_3C_2T_x$ films | 1.1 | 1M $H_2SO_4$ | 499 | $2mV\ S^{-1}$ | 10,000 /100% | 7 |
| N-doped delaminated titanium carbides | 1.8 | 6M KOH | 266.5 | $5mV{\cdot}S^{-1}$ | 2000 /86.4% | 8 |
| Nitrogen-doped d-$Ti_3C_2$ | 1.7 | 6M KOH | 190 | $1A{\cdot}g^{-1}$ | 10,000 /88.9 | 9 |
| MDC-OMC* | 5 | 6M KOH | 249 | $1A{\cdot}g^{-1}$ | 7,000 /98% | 10 |

Note: $C_g$, TAEA, PVA, EMI-TFS, PTFE, RGO, and MDC-OMC respectively denote gravimetric capacitances, tris(2-aminoethyl)amine, poly(vinylalcohol), 1-Ethyl-3-methylimidazolium bis(trifluoromethylsulfonyl)imide, polytetrafluoroethylene, reduced graphene oxide, MXene-derived carbon ($Ti_3C_2T_x$)-ordered mesoporous carbons.

## References


1. Lukatskaya, M. R., Kota, S., Lin, Z. F., Zhao, M. Q., Shpigel, N., Levi, M. D., Halim. J., Taberna, P. L., Barsoum, M. W., Simon, P., and Gogotsi, Y. (2017). Ultra-high-rate pseudocapacitive energy storage in two-dimensional transition metal carbides. *Nat. Energy.* **2**, 17105.

2. Li, J., Yuan, X. T., Lin, C., Yang, Y. Q., Xu, L., Du, X., Xie, J. L., Lin, J.H., and Sun, J. L. (2017). Achieving high pseudocapacitance of 2D titanium carbide (MXene) by cation intercalation and surface modification. *Adv. Energy. Mater.* **7**, 1602725.

3. Ghidiu, M., Lukatskaya, M. R., Zhao, M.-Q., Gogotsi, Y., and Barsoum, M. W. (2014). Conductive two-dimensional titanium carbide 'clay' with high volumetric capacitance. *Nature* **516**, 78–81.

4. Li, T. F., Yao, L. L., Liu, Q. L., Gu, J. J., Luo, R.C., Li, J.H., Yan, X. D., Wang, W. Q., Liu, P., Chen, B., Zhang, W., Abbas, W., Naz, R., and Zhang, D. (2018).Fluorine-Free Synthesis of High-Purity $Ti_3C_2T_x$ (T= OH, O) via Alkali Treatment. *Angew. Chem., Int. Ed.* **57**, 6115-6119.

5. Tian, W. Q., VahidMohammadi, A., Wang, Z., Ouyang, L.Q., Beidaghi, M., and Hamedi, M. M. (2019). Layer-by-layer self-assembly of pillared two-dimensional multilayers. *Nat. Commun.* **10**, 1-10.

6. Lin, Z. F., Barbara, D., Taberna, P. L., Van Aken, K. L., Anasori, B., Gogotsi, Y., and Simon, P. (2016).Capacitance of $Ti_3C_2T_x$ MXene in ionic liquid electrolyte. *J. Power Sources.* **326**, 575-579.

7. Hu, M. M., Li, Z. J., Zhang, H., Hu, T., Zhang, C., Wu, Z., and Wang, X. H. (2015). Self-assembled $Ti_3C_2T_x$ MXene film with high gravimetric capacitance. *Chem. Commun.* **51**, 13531-13533.

8. Yang, C. H., Que, W. X., Yin, X. T., Tian, Y. P., Yang, Y. W., and Que, M. D. (2017). Improved capacitance of nitrogen-doped delaminated two-dimensional titanium carbide by urea-assisted synthesis. *Electrochim. Acta.* **225**, 416-424.

9. Yang, L., Zheng, W., Zhang, P., Chen, J., Zhang, W., Tian, W. B., and Sun, Z. M. (2019). Freestanding nitrogen-doped d-$Ti_3C_2$/reduced graphene oxide hybrid films for high performance supercapacitors. *Electrochim. Acta.* **300**, 349-356.

10. Wang, J., Tang, J., Ding, B., Malgras, V., Chang, Z., Hao, X. D., Wang, Y., Zhang, X. G., and Yamauchi, Y. (2017). Hierarchical porous carbons with layer-by-layer motif architectures from confined soft-template self-assembly in layered materials. *Nat. commun.* **8**, 15717.